Protein Engineering, Design & Selection, 2017, vol. 30 no. 10, pp. 705–712
doi: 10.1093/protein/gzx050
Advance Access Publication Date: 13 October 2017
Original Article

OXFORD

Original Article

Engineering a temperature sensitive tobacco etch virus protease

J. Wong[1], X. Chen[1], and K. Truong[1,2,*]

[1]Institute of Biomaterials and Biomedical Engineering, University of Toronto, 164 College Street, Toronto, Ontario, Canada M5S 3G9, and [2]Edward S. Rogers, Sr. Department of Electrical and Computer Engineering, University of Toronto, 10 King's College Circle, Toronto, Ontario, Canada M5S 3G4

[*]To whom correspondence should be addressed. Room 407, Rosebrugh Building, Toronto, Ontario, Canada M5S 3G9.
E-mail: kevin.truong@utoronto.ca
Edited By: Ashutosh Chilkoti

Received 29 April 2017; Revised 4 August 2017; Editorial Decision 21 August 2017; Accepted 26 August 2017

Abstract

Since tobacco etch virus protease (TEVp) has a high specificity and efficiency in cleaving its target substrates, many groups have attempted to engineer conditional control of its activity. Temperature induction is widely used for modulating gene function because it has fast temporal response, good penetrability and applicability to many model organisms. Here, we engineered a temperature sensitive TEVp (tsTEVp) by using N-terminal truncations to TEVp that achieved efficient proteolysis on a timescale of 4 h after 30°C induction, while remaining relatively inactive at 37°C. As demonstration, tsTEVp was used to generate temperature-induced biological responses for protein translocation, protein degradation and Ca^{2+}-mediated cellular blebbing. Lastly, tsTEVp and their engineered target substrates could find applications in engineered synthetic biological systems.

Key words: biosensor, live cell imaging, temperature sensitive, TEV protease

Introduction

Tobacco etch viruses (TEVs) express all of their proteins in the form of polyproteins before they are cleaved by the TEV nuclear inclusion α protease (TEVp) (Dougherty and Semler, 1993). As TEVp is highly specific and efficient at cleaving its substrates, it has become a popular tool for cleaving genetically engineered fusion proteins, especially in the removal of affinity tags in tandem affinity purification (Phan *et al.*, 2002). Furthermore, the high specificity of TEVp reduces the probability of cleaving off-target proteins and thus allows it to be expressed in a number of model systems such as *Escherichia coli* (Henrichs *et al.*, 2005), *Saccharomyces cerevisiae* (Kohler, 2003), *Drosophia melanogaster* (Pauli *et al.*, 2008), and mammalian cells cultures (Wehr *et al.*, 2006) without adverse effects on development and viability. While TEVp has mostly been expressed separately from the fusion protein that it cleaves, its self-cleavage characteristics has been previously explored in *E. coli* (Shih *et al.*, 2005) and plants (Marcos and Beachy, 1997; Bedoya *et al.*, 2010). To express multiple genes at precise stoichiometry, our group delivered TEVp fused with multiple target genes, requiring TEVp to self-cleave within the polyprotein (Chen *et al.*, 2010).

Various groups have successfully engineered conditional control over TEVp activity. Using a UAS promoter and GAL4 transactivation system, TEVp was expressed in a cell-type-specific manner in *D. melanogaster* to cleave and deactivate an engineered Rad21 protein bearing a TEVp cleavage site (Pauli *et al.*, 2008). Using rapamycin-induced FRB-FKBP12 interaction to assemble split-TEVp fragments, several executioner caspases were activated by reconstituted split-TEVp to induce subsequent apoptosis (Wehr *et al.*, 2006; Williams *et al.*, 2009; Gray *et al.*, 2010). In other work, TEVp was recruited to the plasma membrane (PM) by tethering to a receptor signaling protein following receptor activation (Barnea *et al.*, 2008). The induced-proximity of TEVp allowed it to cleave a weakened TEV substrate and release a transcription factor into the nucleus and activate the transcription of a reporter gene.

Temperature induction is widely used for modulating gene function because it has fast temporal response, good penetrability and applicability to many model organisms (Labib *et al.*, 2000; Tian *et al.*, 2003; Zeidler *et al.*, 2004; Garaigorta *et al.*, 2005; Liang *et al.*, 2007; Vidali *et al.*, 2009; O'Rourke *et al.*, 2011). Typically, a temperature sensitive mutant protein has a marked drop in activity when expressed above a certain temperature (restrictive temperature), while at a lower temperature (permissive temperature), the activity is very similar to the wild-type protein (Chakshusmathi *et al.*, 2004; Mondal *et al.*, 2007; Tan *et al.*, 2009). Temperature induction in biosystems are commonly engineered using heat shock promoters but these promoters have cross activity with other physiological (e.g. hypoxia and energy depletion) and pathological (e.g. viral infection and inflammation) conditions, making responses potentially non-specific to temperature (Kregel, 2002). Here, we engineered a temperature sensitive TEVp (tsTEVp) by N-terminal truncations that achieved efficient proteolysis under 30°C induction, while remaining relatively inactive at 37°C. Then, tsTEVp was used together with other synthetic tools to generate temperature-induced biological responses in mammalian cells for protein translocation, protein degradation and Ca^{2+}-mediated cellular blebbing.

Materials and methods

Construction of expression plasmids

All constructs were subcloned using the fluorescent cassette-based approach (Truong *et al.*, 2003). Cassettes encoding TEVp, TEV substrate (tevS), fluorescent proteins (CFP, YFP and RFP), CaRQ and localization signals (DAGR, LynS and NLS) were obtained from our previous work. Cassettes encoding mutant TEV substrate (tevX) and Degron (Deg) were created by amplifying the Venus gene with custom primers (Invitrogen) containing tevX and Deg overhanging sequences.

Bacterial expression

Transformation was done using DH5α Subcloning Efficiency chemically competent *E. coli* cells (Invitrogen). Transformed cells were cultured in Luria Broth (LB) with 100 μg/ml ampicillin or 80 μg/ml kanamycin. Bacterial colonies were grown on LB agar plates with 200 μg/ml ampicillin. Colonies were observed using the Illumatool Tunable Lighting System (Light Tools Research, Encinitas, CA) using excitation filters (440, 488 and 540 nm) and longpass emission filters (480, 525 and 560 nm for CFP (Cerulean), YFP (Venus) and RFP (mRFP), respectively). Purification of plasmids after bacterial culture was done using the PureLink Quick Plasmid Miniprep kit (Invitrogen).

Cell culture and cell line transfection

Cell lines (COS-7, HEK-293, HeLa and CHO) were cultured in Dulbecco's modified Eagle's medium supplemented with 25 mM D-glucose, 1 mM sodium pyruvate, 4 mM L-glutamine and 10% FBS (Invitrogen) with 100 U/ml penicillin and 100 μg/ml streptomycin (Sigma) in T-25 flasks. Cells were maintained 37°C in a humidified atmosphere containing 5% CO_2. Cells were passaged at 95% confluency with 0.05% trypsin-EDTA (Sigma). Lipofectamine 2000 was used as the transfection reagent (Invitrogen).

Sodium dodecyl sulfate-polyacrylamide gel electrophoresis

Equal amounts of fluorescence-normalized lysates or purified protein solutions were mixed with 1× NuPAGE LDS sample buffer (Invitrogen) to a total volume of 30 μl. The resulting mixture was heated at 70°C for 10 min before they were loaded on NuPAGE Novex 4–12% Bis–Tris pre-cast polyacrylamide gels with 1× SDS-MOPS buffer (Invitrogen). The gels were run on Owl EC-105 Vertical Electrophoresis System (Thermo Scientific) at 120 V for 60–90 min. PageRuler protein ladder (Fermentas) was run simultaneously and used for size reference. Gels were stained overnight in PageBlue Comassie blue-based stain (Fermentas) to visualize protein ladder. Fluorescent bands were visualized using Illumatool system, with appropriate excitation and emission filters as previously mentioned. Photographs of the fluorescent bands are taken by a Canon A350 Powershot camera.

Live cell imaging

Imaging experiments were conducted in cell culture medium, except for ATP experiments where PBS supplemented with 1 mM Ca^{2+} was used. Stimulatory reagents were added directly by diluting 1:10 in imaging medium. For experiments where stimulants were added, 200 μl of 10× concentration were added dropwise around wells to improve even diffusion throughout the dish. The following stimulatory reagents were used at the indicated concentration: PDBu (10 μM, Sigma), ATP (10 μM, Fermentas), ionomycin (1 μM, Sigma), $CaCl_2$ (1 mM, Sigma), staurosporine (2 μM, Sigma). All reagents with the exception of $CaCl_2$ and ATP were prepared in DMSO stocks.

Imaging was performed using an inverted IX-81 microscope (Olympus, Markham ON) with a Lambda DG4 xenon lamp and QuantEM 512SC CCD camera. Bandpass filters (Semrock, Rochester, NY) for CFP, YFP and RFP excitation were 438/24, 500/24 and 580/20 nm, respectively, and for emission were 482/32, 542/27 and 630/60 nm, respectively. Image acquisition and analysis were done using MetaMorph Advanced.

Data analysis

All experiments were performed at least in triplicates, and graphed data are presented as mean ± standard deviation, unless otherwise stated. For comparing means, significance was calculated using unpaired Student's *t*-test assuming equal variance. For comparing medians, Kruskal–Wallis test was used. $P < 0.05$ was considered significant.

Ratiometric quantification of fluorescent proteins

Nucleus to PM (Nuc/Mem) ratios for the TEVpSensor was calculated by the following formula:

$$\text{Nuc/Mem} = \frac{I_{\text{CFP(nucleus)}}}{I_{\text{RFP(nucleus)}}} \Big/ \frac{I_{\text{CFP(membrane)}}}{I_{\text{RFP(membrane)}}}$$

where I_{CFP} and I_{RFP} are background-corrected average pixel intensities of CFP and RFP, respectively, within the indicated region of interest (nucleus or membrane). For N-degron reporters, unnormalized YFP and RFP values were background-corrected average pixel intensities of the cytoplasm. YFP/RFP values were normalized to the average YFP/RFP value of RFP-tevX-Deg-YFP when expressed on its own.

Results and discussion

Creation of tsTEVp by incremental N-terminal shortening

N-terminal truncations to TEVp yielded a variant named tsTEVp that achieved efficient proteolysis on a timescale of 4 h after 30°C induction, while remaining relatively inactive at 37°C (Fig. 1, S1, S2, S3). While temperature sensitive mutants can be created by random mutagenesis (Chakshusmathi *et al.*, 2004), the method of N-terminal truncations was used in this study on the basis of two previous findings: first, incremental truncations can result in stepwise reduction of activity (Haruki *et al.*, 1994; Vainshtein *et al.*, 1996; Trevino *et al.*, 1998; Van der Schueren *et al.*, 1998; Yang *et al.*, 2001; Hecky and Muller, 2005; Alone *et al.*, 2007); second, TEVp has an innate temperature sensitivity with peak enzymatic activity at 30°C (Nallamsetty *et al.*, 2004; Raran-Kurussi *et al.*, 2013). Consequently, TEVp was incrementally truncated at the N-terminal to discover variants where the activity is negligible at 37°C, but sufficiently retained at 30°C. To measure TEVp activity, a biosensor (named TEVpSensor) was created as a tandem fusion of a PM localization signal (^{1}MGCIKSKGKDSA^{12} from Lyn kinase) (LynS), monomeric red fluorescent protein (RFP), the canonical TEVp recognition site ENLYFQS (tevS), cyan fluorescent protein (CFP) and a nuclear localization sequence (NLS) (^{6}RIRKKLR^{12} from DNA primase (Mizuno *et al.*, 1996)) (Fig. S1). In the presence of TEVp activity, CFP will be released from the PM and translocate into the nucleus, creating a distinct fluorescence distribution (Fig. S1B). In the absence of TEVp activity, illustrated by TEVpSensor co-expressed with the catalytically inactive tsTEVp(C151A) mutant, both RFP and CFP will be tethered to the PM (Fig. S1C).

The activity of each truncated TEVp variant was assayed with the co-expression of TEVpSensor in COS-7 cells (Fig. S2). Following a one-day posttransfection period at 37°C, the proteolytic activity of each variant was assessed by the proportion of transfected cells displaying a cleaved sensor (judged by a clear CFP-stained nucleus). The deletion of the first 13 residues did not have a noticeable impact on the catalytic activity of TEVp (Fig. S2A). From S15 TEVp onwards, the catalytic activity was significantly reduced, while H20 TEVp and H21 TEVp did not register any activity within the experimental time frame and temperature conditions. The greatest drop in catalytic activity occurred at I18TEVp (Δ1–17), which was also where the first β-strand residue was removed (Thr17). Each variant was then subjected to a further 4-h incubation at both 30°C and 37°C. Consequently, the catalytic efficiency for the five consecutive truncations from S15 TEVp to C19 TEVp displayed temperature dependence, with all of them registering higher activity at 30°C than at 37°C (Fig. S2B). The background activity of S15 TEVp, S16 TEVp and T17 TEVp were large with over 50% of the cells displaying a cleaved sensor at 37°C. In contrast, the activity of T19 TEVp was well suppressed at 37°C but could only be marginally activated by lowering the temperature to 30°C. Since I18TEVp displayed the greatest contrast in activity between the two temperatures and the background activity of I18TEVp remained suppressed at 37°C over a course of 16 h (Fig. S2C), it was selected as the temperature sensitive TEVp (hereafter, tsTEVp). Sodium dodecyl sulfate-polyacrylamide gel electrophoresis analysis of lysates extracted from COS-7 cells expressing tsTEVp and TEVpSensor presented further evidence of temperature-dependent activity of tsTEVp (I18TEVp) (Fig. S2D). The two bands shown are for the full length TEVpSensor at ~50 kDa and the RFP component of the cleaved TEVpSensor (LynS-RFP) at ~25 kDa. Background cleavage at 37°C was evident, but well suppressed within 16 h after induction, as indicated by a much fainter band at LynS-RFP level than at TEVpSensor level. Cleavage proceeded towards completion after 16 h at 30°C as indicated by disappearance of the band at TEVpSensor size. Temperature-dependent activity of tsTEVp was also observed in HEK-293, HeLa and CHO cells which indicates that tsTEVp is not cell-type specific (Fig. S3). Lastly, the kinetic parameters K_M and k_{cat} for tsTEVp were determined using protein substrates containing tevS (Table I).

Sequential translocation from nucleus to membrane mediated by tsTEVp and DAGR

A target protein can be sequentially routed from the nucleus to the cytoplasm and then from the cytoplasm to the PM by combining two synthetic inputs: (1) temperature-induced translocation by tsTEVp activity and (2) PDBu (phorbol 12,13-dibutyrate)-induced translocation by DAGR (DAG reporter, Cys1 domain of PKC β–isoform) (Violin *et al.*, 2003) (Fig. 2). Within the construct of CFP-NLS-tevS-DAGR-YFP-NES, YFP is the target protein for translocation (Fig. 2A). YFP will be originally localized within nucleus by the presence of NLS but can be moved to the PM by a two-step process. First, the temperature-induced cleavage at tevS by tsTEVp will result in the separation of DAGR-YFP-NES from CFP-NLS and its release into the cytoplasm by a nuclear export signal (NES). Second, addition of PDBu will allow recruitment of DAGR to membrane-bound DAG (diacylglycerol) molecules, thereby directing YFP to the PM. A 4-h incubation at 30°C resulted in 57 ± 13% of COS-7 cells co-expressing CFP-NLS-tevS-DAGR-YFP-NES and tsTEVp to display a differential localization of CFP and YFP between the nucleus and the cytoplasm (Fig. 2B and C). Both CFP and YFP were nuclear localized in most of the cells maintained at 37°C for the same duration. The addition of PDBu triggered the secondary translocation event where cytoplasmic DAGR-YFP migrated to the PM, typically within 2 to 5 min (Fig. 2C). This event was visible in all cells with a sufficient cytoplasmic concentration of DAGR-YFP-NES (i.e. most of the cells in 30°C-induced cultures). Cells maintained at 37°C did not display PM-localized DAGR-YFP after PDBu-induction. Instead, the entire construct CFP-NLS-tevS-DAGR-YFP-NES formed a perimeter around the nucleus, a phenomena likely caused by the binding to DAG molecules present on the nuclear membrane (Fig. 2D).

tsTEVp- mediated protein degradation by N-degron activation

Temperature-dependent protein degradation was achieved by using tsTEVp to activate a dormant N-degron (Fig. 3, S4). The N-degron is a class of degrons where the N-terminal sequence of a protein determines its *in vivo* stability (Ravid and Hochstrasser, 2008). In eukaryotes, the N-degron consists of a destabilizing N-terminal residue (Cys, Arg, His, Lys, Leu, Phe, Trp, Tyr or Ile) (Ravid and Hochstrasser, 2008), followed by an internal Lys residue for polyubiquitination (Varshavsky, 1996; Mogk *et al.*, 2007). The enzymatic activity of TEVp is flexible towards the last residue (X) of its 7-residue recognition sequence (ENLYFQ-X), which becomes the new N-terminal residue after proteolytic cleavage (Kapust *et al.*, 2002). By placing a destabilizing residue at X, the new downstream fragment following TEVp cleavage will become susceptible to N-degron mediated degradation, as first demonstrated in yeast by Taxis *et al.* (2009). This study presents a conditional degradation mechanism determined by temperature-induced activity of tsTEVp. YFP was

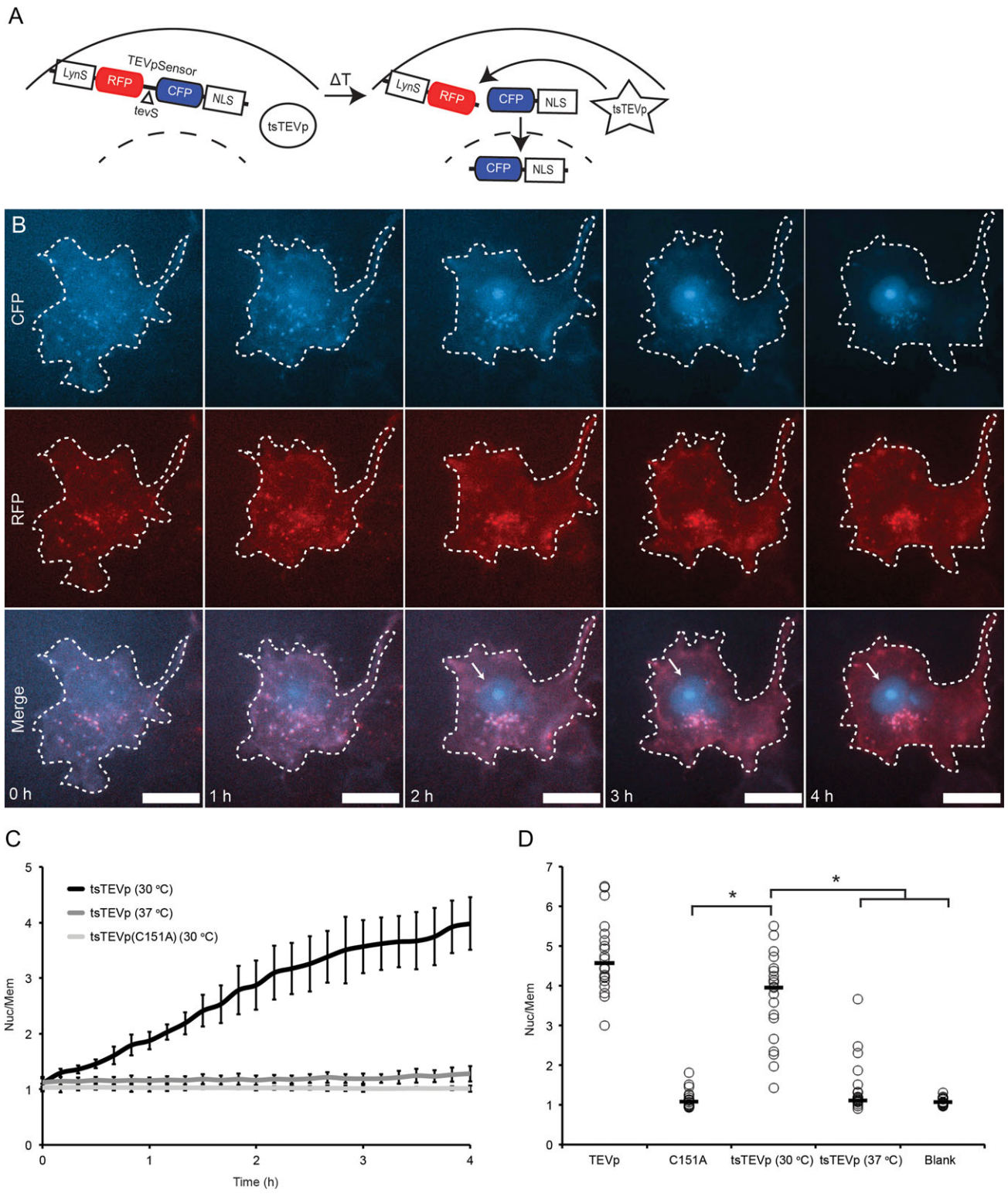

Fig. 1 Quantitative analysis of tsTEVp activity using TEVpSensor. (**A**) Cartoon representation of how tsTEVp activity can be detected by translocation of TEVpSensor. (**B**) Progression of tsTEVp activity as indicated by TEVpSensor. Arrow indicates visible nuclear staining by CFP after 2 h. Scale bars represent 30 μm. COS-7 cell outlines are marked by dashed lines in selected panels. (**C**) Time-lapse quantification of TEVpSensor cleavage under indicated expression and temperature conditions (data are mean ± SD, $n = 3$). (**D**) Scatter plot showing Nuc/Mem values of individual cells (hollow circles) transfected with indicated construct along with TEVpSensor. The cells were incubated for 4 h at 37°C unless indicated otherwise. Solid line represents the median ($n = 20$ cells, $^*P < 0.001$).

Table I. Kinetic parameters for wild-type TEVp and tsTEVp

Enzyme	Temperature (°C)	K_M (mM)	k_{cat} (s^{-1})	k_{cat}/K_M ($mM^{-1}\,s^{-1}$)
Wild-type TEVp	30	0.049 ± 0.012	0.18 ± 0.01	3.67 ± 0.50
tsTEVp	30	0.066 ± 0.010	0.16 ± 0.01	2.42 ± 0.40
tsTEVp	30[a]	0.066 ± 0.010	0.16 ± 0.01	2.42 ± 0.40

[a]tsTEVp was incubated in 30°C for 30 min, then 37°C for 30 min before measurement.

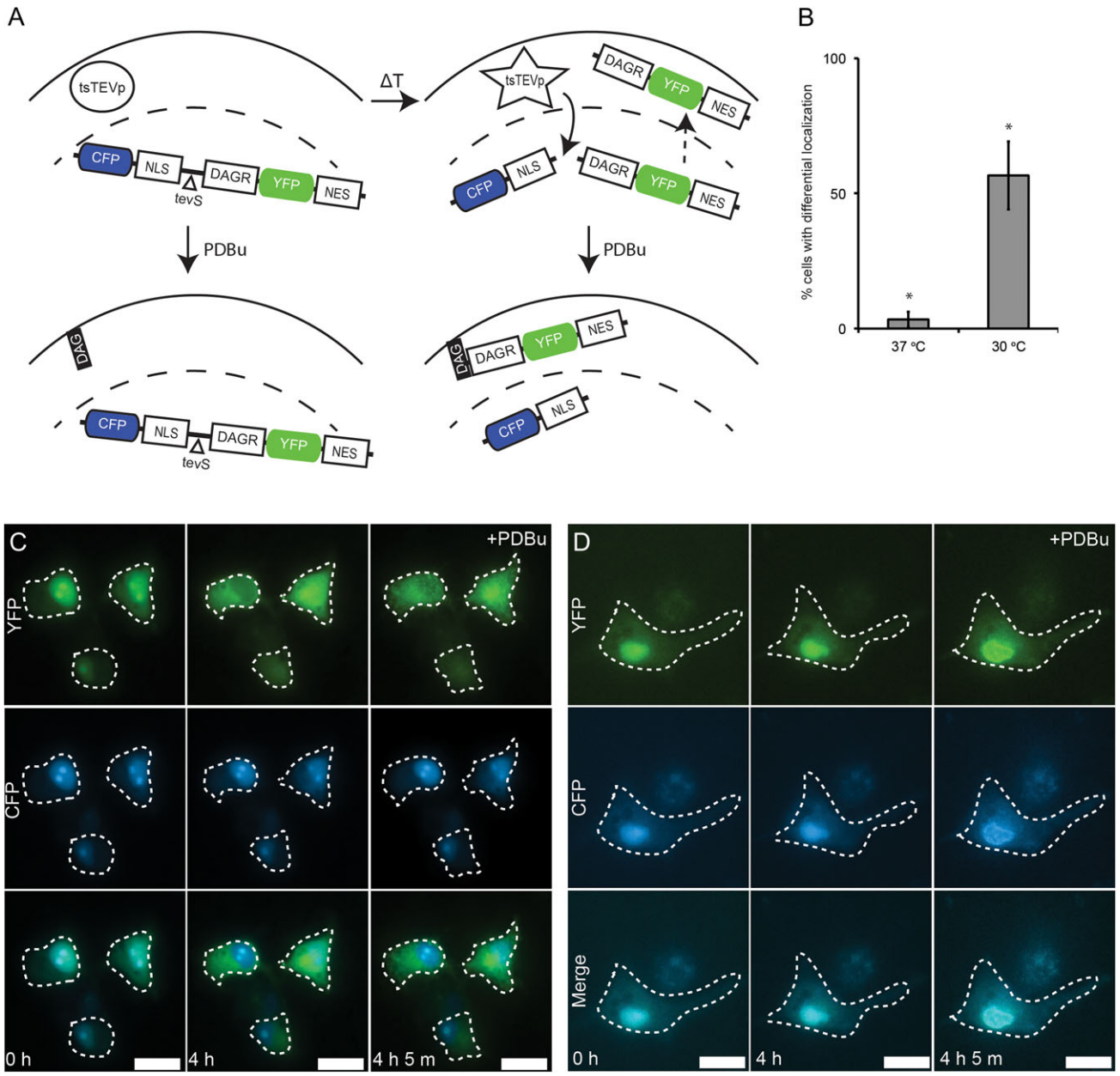

Fig. 2 tsTEVp and DAGR mediated protein translocation. (**A**) Cartoon representation of how a target protein (YFP) can be released from nuclear confinement and rerouted to the PM. (**B**) Percent COS-7 cells co-expressing CFP-NLS-tevS-DAGR-YFP-NES and tsTEVp displaying differential localization of YFP and CFP after 4-hour incubation at indicated temperature (data are mean ± SD, $n = 3$ experiments/20 cells each, $^*P < 0.01$). (**C**) Representative images showing 30°C-induced release of YFP into the cytoplasm and subsequent PDBu-induced membrane localization. (**D**) Representative images showing nuclear-confined YFP in the absence of temperature induction, followed by ineffective PDBu-induction. Scale bars represent 30 μm. Cell outlines are marked by dashed lines in selected panels.

used as a target of degradation by fusing with RFP-tevX-Deg to yield a fluorescent reporter in the form of RFP-tevX-Deg-YFP (Fig. S4). tevX are TEVp recognition sites with alternative residues (X) in place of Ser of tevS, and Deg is an unstructured peptide sequence which harbors an internal Lys residue for polyubiquitination (Taxis *et al.*, 2009). The cleavage of the reporter at tevX creates

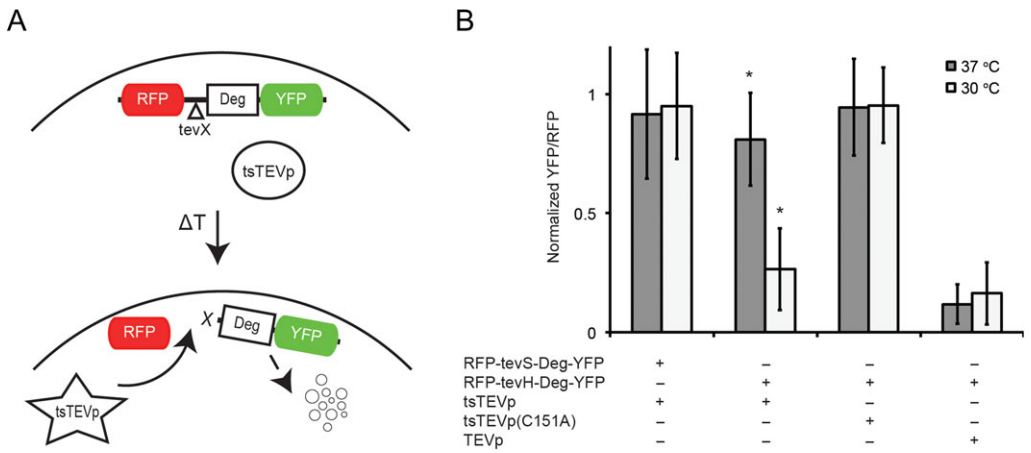

Fig. 3 Synthetic activation of protein degradation by tsTEVp. (**A**) Cartoon representation of temperature-dependent protein degradation following N-degron exposure. (**B**) Normalized YFP/RFP values of COS-7 cells co-expressing the indicated proteins under different temperature conditions temperature (data are mean ± SD, $n = 48$ cells, $^*P < 0.001$). The YFP/RFP values are normalized to the average YFP/RFP value when RFP-tevH-Deg-YFP or RFP-tevS-Deg-YFP was expressed on their own.

two fragments, RFP and X-Deg-YFP, where X becomes the new N-terminal residue of the downstream fragment.

RFP-tevH-Deg-YFP was selected to analyze the capability of tsTEVp to activate degradation (Fig. 3). The extent of degradation was estimated by the ratio between YFP and RFP quantified from fluorescence microscopy. The ratios were normalized to the YFP/RFP ratio of the fluorescent reporters (RFP-tevH-Deg-YFP and RFP-tevS-Deg-YFP) without co-transfection of the derivatives of TEVp. Therefore, a ratio of one represents either an uncleaved reporter, or a cleaved reporter without differential degradation between RFP and YFP components. There was significantly higher YFP/RFP ratio after 1-day at 30°C than at 37°C ($P < 0.001$) when RFP-tevH-Deg-YFP was co-transfected with tsTEVp (Fig. 3B). When RFP-tevS-Deg-YFP was used, the YFP/RFP ratio remained unchanged (Fig. 3B). This indicates that the stability of Deg-YFP was dependent on the nature of its N-terminal residue, which was conditionally exposed at 30°C by tsTEVp activity.

Cellular blebbing mediated by tsTEVp-controlled localization of CaRQ

Using tsTEVp to alter the localization of CaRQ (i.e. a synthetic Ca^{2+}-sensitive RhoA (Mills and Truong, 2011), the property of Ca^{2+} mediated cellular blebbing endowed by CaRQ was controlled by temperature induction (Fig. 4). Since CaRQ has a lower affinity for Ca^{2+} with an EC_{50} of 27 μM, it cannot be activated to cause cellular blebbing by cytoplasmic Ca^{2+} signals that peak at ~1 μM (Mills and Truong, 2011). CaRQ requires localization to the PM where Ca^{2+} influx concentration near Ca^{2+} channels are high enough to activate CaRQ and trigger cellular blebbing. Thus, the property of Ca^{2+}-mediated cellular blebbing endowed by CaRQ can be modulated by changing the localization by tsTEVp. In the construct LynS-tevS-CaRQ, CaRQ will be localized either on the PM (by LynS) or the cytoplasm depending on TEVp activity (Fig. 4A). When LynS-tevS-CaRQ was co-expressed with tsTEVp in HEK-293, the differential localization of CaRQ became temperature dependent. Only 28.3 ± 10.4% of cells which experienced a 4-h 30°C-incubation displayed membrane-localized CaRQ compared to almost all of cells maintained at 37°C (Fig. 4B, C and D). Following an ATP stimulus that induces a Ca^{2+} transient via IP3-mediated Ca^{2+} release from the endoplasmic reticulum (ER) (Ralevic and Burnstock, 1998), 26.7 ± 2.9% of the cells maintained at 37°C responded to ATP induction by displaying blebbing morphology within 20 min (Fig. 4B and E). This value is not significantly different ($P > 0.5$) from the positive control, LynS-CaRQ, where CaRQ was PM localized under all conditions (Fig. 4E). If the ER empties sufficiently, it will turn on store-operated Ca^{2+} entry through Orai1 channels on the PM. As store-operated Ca^{2+} entry is not guaranteed to happen on ATP stimulus, CaRQ may not necessarily activate. Nonetheless, blebbing was significantly reduced to 6.7 ± 2.9% in 30°C-induced cells, consistent with the depletion of CaRQ from the PM following tsTEVp activity (Fig. 4E). This value is not significantly different ($P > 0.5$) from the negative control, CaRQ. In similar experiments, LOVS1K and Orai1 were co-expressed using a single DualCMV vector ($DualCMV_{LOVS1K/Orai1}$) because LOVS1K can generate local Ca^{2+} influx from Orai1 following blue light stimulation (Mills and Truong, 2013). After 1 min of blue light excitation (i.e. 1 s exposure every 10 s), blebbing was observed in 91.7 ± 7.6% of the HEK-293 cells expressing $DualCMV_{LOVS1K/Orai1}$, tsTEVp and LynS-tevS-CaRQ at 37°C (Fig. 4E). Since LOVS1K turns on Orai1 channels, so it can robustly turn on PM-localized CaRQ at levels near 100%. Only 13.3 ± 10.4% of the 30°C-induced cells were blebbing after the same dosage of blue light (Fig. 4E). Finally, to verify that LynS-tevS-CaRQ can be activated by Ca^{2+} regardless of localization, ionomycin was added to stimulate a period of high Ca^{2+} influx into the cytoplasm (Fig. 4E). Ionomycin is a Ca^{2+} ionophore which allows extracellular Ca^{2+} (in ~1 mM range) to flood into the cell and therefore will activate CaRQ regardless of localization. The activation is not complete as some cells may be dying from the stimulus.

Conclusion

The irreversible modification of proteins by proteolytic cleavage represents a simple and ubiquitous mechanism for signal propagation in living cells, and governs important biological processes such as cell proliferation, development, apoptosis, immunity, blood clotting, and wound healing (Turk, 2006; Doucet and Overall, 2008). To allow for temperature inducible control of proteolytic cleavage, we engineered tsTEVp which has efficient proteolysis under 30°C induction, while remaining relatively inactive at 37°C. Then,

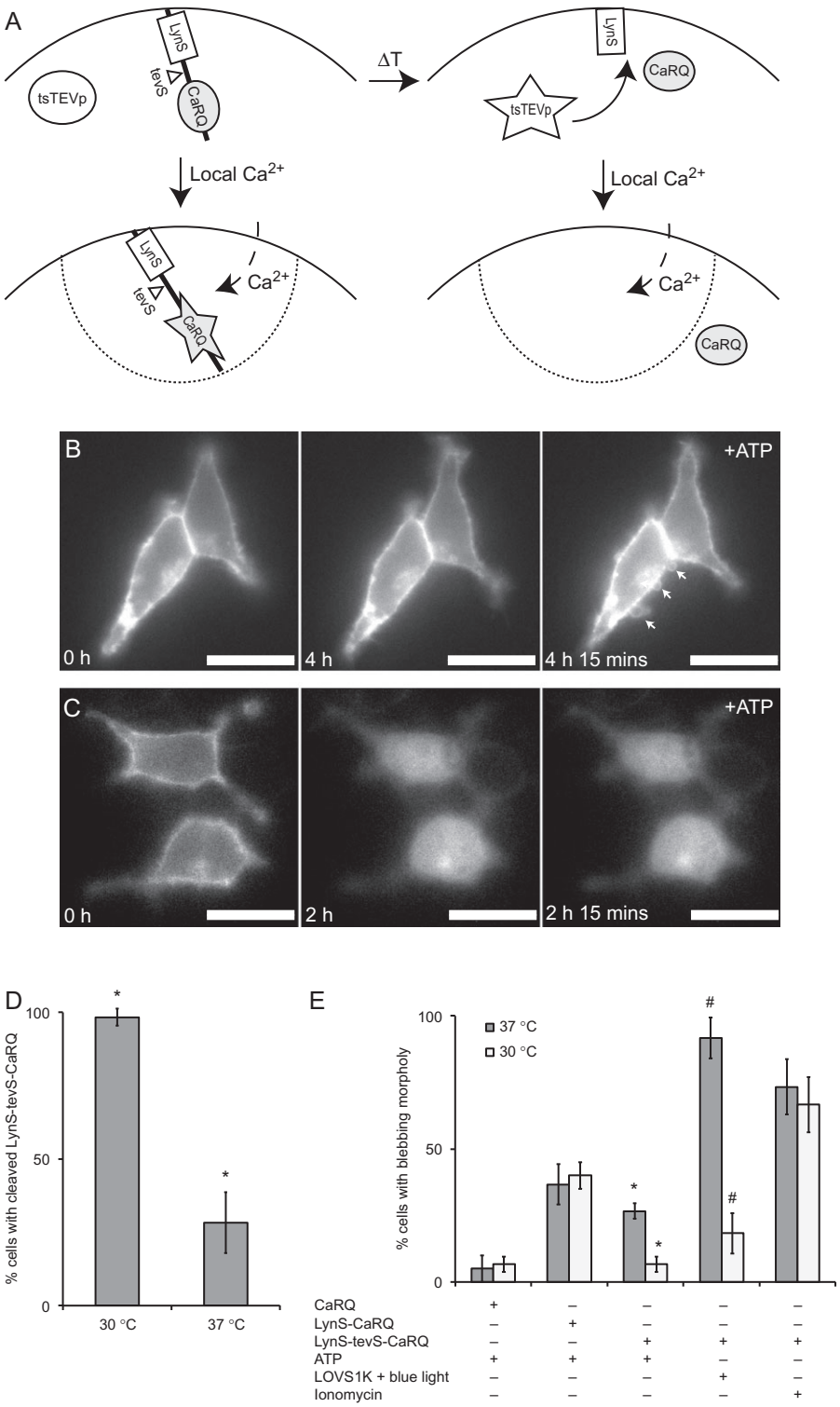

Fig. 4 tsTEVp and CaRQ mediated control over cell blebbing. (**A**) Cartoon representation of using tsTEVp to alter the localization of CaRQ, thereby modulating its sensitivity towards local Ca^{2+} signals. (**B**) HEK-293 cells expressing pLyn-tevS-CaRQ (shown) and tsTEVp incubated at 37°C. ATP was added at 4 h. (**C**) HEK-293 cells expressing pLyn-tevS-CaRQ (shown) and tsTEVp incubated at 30°C. Cleavage of pLyn-tevS-CaRQ appeared to be complete at 2 h. ATP was added at 2 h. (**D**) Percent HEK-293 cells co-expressing pLyn-tevS-CaRQ and tsTEVp displaying membrane-localized CaRQ after 4-h incubation at indicated temperature (data are mean ± SD, $n = 3$ experiments/20 cells each, $^{*}P < 0.001$). (**E**) Percent cells with blebbing morphology under each expression and stimulation conditions (data are mean ± SD, $n = 3/15$, $^{*}P < 0.01$, $^{\#}P < 0.001$).

tsTEVp was combined with other engineered proteins to impart temperature inducibility to protein translocation, protein degradation and Ca^{2+}-mediated cellular blebbing. Considering the functional relevance of proteases in biology and the excellent tissue penetration of temperature induction, tsTEVp and their engineered target substrates could find therapeutic applications in engineered synthetic biological systems. For therapeutic induction of tsTEVp-based genetic circuits *in vivo*, low body temperatures could be achieved by a number of methods including cooling catheters, cooling blankets and ice baths. In fact, induced hypothermia to body temperatures as low as 30°C to 32°C in the timescale of hours is an established therapeutic intervention for acute traumatic injuries such as cardiac arrest (Nolan *et al.*, 2003), stroke (Florian *et al.*, 2008) and brain injuries (Arcure and Harrison, 2009) because the low temperatures slow down cell death processes that would otherwise be more lethal. Future work will involve the engineering of appropriate TEVp target substrates that could be implemented along with tsTEVp to elicit desired temperature-induced biological effects.

Supplementary data

Supplementary data are available at *Protein Engineering, Design and Selection* online.

Acknowledgements

X.C. carried out the initial experiments, created plasmids and co-wrote the manuscript. J.W. continued the work, analyzed the data and co-wrote the manuscript. K.T. conceived the initial idea, analyzed the data and co-wrote the manuscript.

Funding

This work was funded by grants from the Canadian Cancer Society Research Institute (#701936) and Natural Sciences and Engineering Research Council of Canada (NSERC) (#05322-14).

Conflict of interest

None declared.

References

Alone,P.V., Malik,G., Krishnan,A. and Garg,L.C. (2007) *Proc. Natl Acad. Sci. U.S.A.*, **104**, 16056–16061.
Arcure,J. and Harrison,E.E. (2009) *J. Spec. Oper. Med.*, **9**, 22–25.
Barnea,G., Strapps,W., Herrada,G., Berman,Y., Ong,J., Kloss,B., Axel,R. and Lee,K.J. (2008) *Proc. Natl Acad. Sci. U.S.A.*, **105**, 64–69.
Bedoya,L., Martinez,F., Rubio,L. and Daros,J.A. (2010) *J. Biotechnol.*, **150**, 268–275.
Chakshusmathi,G., Mondal,K., Lakshmi,G.S., Singh,G., Roy,A., Ch,R.B., Madhusudhanan,S. and Varadarajan,R. (2004) *Proc. Natl Acad. Sci. U.S.A.*, **101**, 7925–7930.
Chen,X., Pham,E. and Truong,K. (2010) *Protein Sci.*, **19**, 2379–2388.
Doucet,A. and Overall,C.M. (2008) *Mol. Aspects Med.*, **29**, 339–358.
Dougherty,W.G. and Semler,B.L. (1993) *Microbiol. Rev.*, **57**, 781–822.
Florian,B., Vintilescu,R., Balseanu,A.T., Buga,A.M., Grisk,O., Walker,L.C., Kessler,C. and Popa-Wagner,A. (2008) *Neurosci. Lett.*, **438**, 180–185.
Garaigorta,U., Falcon,A.M. and Ortin,J. (2005) *J. Virol.*, **79**, 15246–15257.
Gray,D.C., Mahrus,S. and Wells,J.A. (2010) *Cell*, **142**, 637–646.
Haruki,M., Noguchi,E., Akasako,A., Oobatake,M., Itaya,M. and Kanaya,S. (1994) *J. Biol. Chem.*, **269**, 26904–26911.
Hecky,J. and Muller,K.M. (2005) *Biochemistry*, **44**, 12640–12654.
Henrichs,T., Mikhaleva,N., Conz,C., Deuerling,E., Boyd,D., Zelazny,A., Bibi, E., Ban,N. and Ehrmann,M. (2005) *Proc. Natl Acad. Sci. U.S.A.*, **102**, 4246–4251.
Kapust,R.B., Tozser,J., Copeland,T.D. and Waugh,D.S. (2002) *Biochem. Biophys. Res. Commun.*, **294**, 949–955.
Kohler,F. (2003) *Nucleic Acids Res.*, **31**, doi: ARTN e16, 10.1093/nar/gng016.
Kregel,K.C. (2002) *J. Appl. Physiol. (1985)*, **92**, 2177–2186.
Labib,K., Tercero,J.A. and Diffley,J.F.X. (2000) *Science*, **288**, 1643–1647.
Liang,R.B., Liu,X.P., Liu,J.H., Ren,Q.S., Liang,P.J., Lin,Z.X. and Xie,X.M. (2007) *J. Microbiol. Methods*, **68**, 497–506.
Marcos,J.F. and Beachy,R.N. (1997) *J. Gen. Virol.*, **78**, 1771–1778.
Mills,E. and Truong,K. (2011) *Chem. Biol.*, **18**, 1611–1619.
Mills,E. and Truong,K. (2013) *Cell. Calcium*, **53**, 231–240.
Mizuno,T., Okamoto,T., Yokoi,M., Izumi,M., Kobayashi,A., Hachiya,T., Tamai,K., Inoue,T. and Hanaoka,F. (1996) *J. Cell. Sci.*, **109**, 2627–2636.
Mogk,A., Schmidt,R. and Bukau,B. (2007) *Trends Cell. Biol.*, **17**, 165–172.
Mondal,K., Dastidar,A.G., Singh,G., Madhusudhanan,S., Gande,S.L., VijayRaghavan,K. and Varadarajan,R. (2007) *J. Mol. Biol.*, **370**, 939–950.
Nallamsetty,S., Kapust,R.B., Tozser,J., Cherry,S., Tropea,J.E., Copeland,T.D. and Waugh,D.S. (2004) *Protein Expr. Purif.*, **38**, 108–115.
Nolan,J.P., Morley,P.T., Vanden Hoek,T.L. *et al.* (2003) *Circulation*, **108**, 118–121.
O'Rourke,S.M., Carter,C. and Carter,L. *et al.* (2011) *PLoS ONE*, **6**, doi: ARTN e16644.
Pauli,A., Althoff,F., Oliveira,R.A., Heidmann,S., Schuldiner,O., Lehner,C.F., Dickson,B.J. and Nasmyth,K. (2008) *Dev. Cell.*, **14**, 239–251.
Phan,J., Zdanov,A., Evdokimov,A.G., Tropea,J.E., Peters,H.K., Kapust,R.B., Li,M., Wlodawer,A. and Waugh,D.S. (2002) *J. Biol. Chem.*, **277**, 50564–50572.
Ralevic,V. and Burnstock,G. (1998) *Pharmacol. Rev.*, **50**, 413–492.
Raran-Kurussi,S., Tozser,J., Cherry,S., Tropea,J.E. and Waugh,D.S. (2013) *Anal. Biochem.*, **436**, 142–144.
Ravid,T. and Hochstrasser,M. (2008) *Nat. Rev. Mol. Cell. Biol.*, **9**, 679–690.
Shih,Y.P., Wu,H.C., Hu,S.M., Wang,T.F. and Wang,A.H.J. (2005) *Protein Sci.*, **14**, 936–941.
Tan,G.H., Chen,M., Foote,C. and Tang,C.G. (2009) *Genetics*, **183**, 13–22.
Taxis,C., Stier,G., Spadaccini,R. and Knop,M. (2009) *Mol. Syst. Biol.*, **5**, 267.
Tian,J., Yam,C., Balasundaram,G., Wang,H., Gore,A. and Sampath,K. (2003) *Development*, **130**, 3331–3342.
Trevino,R.J., Tsalkova,T., Kramer,G., Hardesty,B., Chirgwin,J.M. and Horowitz,P.M. (1998) *J. Biol. Chem.*, **273**, 27841–27847.
Truong,K., Khorchid,A. and Ikura,M. (2003) *BMC Biotechnol.*, **3**, 8.
Turk,B. (2006) *Nat. Rev. Drug Discov.*, **5**, 785–799.
Vainshtein,I., Atrazhev,A., Eom,S.H., Elliott,J.F., Wishart,D.S. and Malcolm, B.A. (1996) *Protein Sci.*, **5**, 1785–1792.
Van der Schueren,J., Robben,J. and Volckaert,G. (1998) *Protein Eng.*, **11**, 1211–1217.
Varshavsky,A. (1996) *Proc. Natl Acad. Sci. U.S.A.*, **93**, 12142–12149.
Vidali,L., Augustine,R.C., Fay,S.N., Franco,P., Pattavina,K.A. and Bezanilla, M. (2009) *Plant Physiol.*, **151**, 506–514.
Violin,J.D., Zhang,J., Tsien,R.Y. and Newton,A.C. (2003) *J. Cell. Biol.*, **161**, 899–909.
Wehr,M.C., Laage,R., Bolz,U., Fischer,T.M., Grunewald,S., Scheek,S., Bach, A., Nave,K.A. and Rossner,M.J. (2006) *Nat. Methods*, **3**, 985–993.
Williams,D.J., Puhl,H.L. and Ikeda,S.R. (2009) *PLoS ONE*, **4**, doi: ARTN e7474, 10.1371/journal.pone.0007474.
Yang,F., Cheng,Y., Peng,J., Zhou,J. and Jing,G. (2001) *Eur. J. Biochem.*, **268**, 4227–4232.
Zeidler,M.P., Tan,C., Bellaiche,Y., Cherry,S., Hader,S., Gayko,U. and Perrimon,N. (2004) *Nat. Biotechnol.*, **22**, 871–876.